Electronic supplementary information

Enabling Efficient Near-infrared Emission in Lead-free Double Perovskite via a Codoping Strategy

Xiangyan Yun[1,2], Hanlin Hu[3], Haizhe Zhong[2], Jingheng Nie[4,*], Henan Li[5], Yumeng Shi[1,5*]

[1] Key Laboratory of Luminescence and Optical Information Ministry of Education Institute of Optoelectronic Technology, Beijing Jiaotong University, Beijing 100044, P. R. China

[2] International Collaborative Laboratory of 2D Materials for Optoelectronics Science and Technology of Ministry of Education, Institute of Microscale Optoelectronics, Shenzhen University, Shenzhen 518060, P. R. China

[3] Hoffman Institute of Advanced Materials, Shenzhen Polytechnic, Shenzhen 518060, P. R. China

[4] Guangdong Rare Earth Photofunctional Materials Engineering Technology Research Center, School of Chemistry and Environment, Jiaying University, Meizhou, 514015, P. R. China

[5] School of Electronics and Information Engineering, Shenzhen University, Shenzhen 518060, P. R. China

*J. N. E-mail: niejh@jyu.edu.cn

*Y. S. E-mail: ymshi@bjtu.edu.cn

Experimental Section

Materials: CsCl (99.99% metals basis) was purchased from Shanghai Aladdin Biochemical Co., Ltd. NaCl (99.99% metals basis), $InCl_3$ (99.99% metals basis), $SbCl_3$ (99.9% metals basis) and Anhydrous ethanol were purchased from Shanghai Macklin Biochemical Technology Co., Ltd. $YbCl_3·6H_2O$ (99.9% metals basis) and $NdCl_3·6H_2O$ (99.9% metals basis) were purchased from Shanghai Bide Pharmatech Co., Ltd. All chemicals were used as received without any further purification.

Growth of $Cs_2NaInCl_6$ and Sb^{3+}-Ln^{3+} (Ln = Yb^{3+}, Nd^{3+}) Co-doped $Cs_2NaInCl_6$ Single crystals

Pristine and Sb^{3+}-Ln^{3+} (Ln = Yb^{3+}, Nd^{3+})-codoped $Cs_2NaInCl_6$ single crystals were synthesized by a simple solvothermal method. Synthesis for $Cs_2NaInCl_6$, 2.4 mmol (0.404 g) CsCl, 1.2 mmol (0.0695 g) NaCl, 1.2 mmol (0.2654 g) $InCl_3$, and 10 mL HCl were transferred into a Teflon autoclave (25 mL). After sealing, it was subsequently placed in a drying oven and kept at 180 °C for 12 h, and then the temperature was lowered with a rate of 3.3 °C h^{-1}. The centimeter-sized single-crystal particles of $Cs_2NaInCl_6$ were obtained after about 2.5 days. After the experiment is completed, remove the sealed Teflon autoclave. Then, extract the hydrochloric acid solution from it, add an appropriate amount of ethanol, and transfer the single crystals to a glass Petri dish for cleaning. Repeat this cleaning process three times. Place the Petri dish in a drying oven (65 °C) and remove it after half an hour. For the Sb^{3+}-Ln^{3+} (Ln = Yb^{3+}, Nd^{3+})-codoped $Cs_2NaInCl_6$ single crystals, the same method was used. The amount of CsCl, NaCl, and hydrochloric acid solution remain unchanged, and different proportions of $InCl_3$, $SbCl_3$ (99.9% metals basis), $YbCl_3·6H_2O$, and $NdCl_3·6H_2O$ were added.

Fabrication of NIR LEDs: 1.8 g of the $Cs_2NaInCl_6$:Sb^{3+},Yb^{3+} powder samples were dispersed into 1.8 g of complex gums, the thoroughly mixed mixture is transferred onto the surfaces of multiple LED chips (Zhongke Haoye (Dongguan) Material Technology Co., Ltd.) with emission wavelengths of 365 nm, and cured in an oven for 1.5 h.

Characterization: PXRD measurements of Sb^{3+}/Ln^{3+}-codoped $Cs_2NaInCl_6$ samples were performed on a Bruker D2 diffractometer (30 kV, 15 mA) equipped with Cu-Kα radiation tubes (λ = 1.5418 Å). For Sb^{3+}/Ln^{3+}-codoped $Cs_2NaInCl_6$ powders, the optical UV−VIS absorption spectra were measured by a UV-2600i spectrophotometer over the spectral range 200-850 nm. ICP-MS was performed on American Agilent 720ES. SEM and EDS were recorded on Czech TESCAN MIRA LMS. The PL, PLE, and lifetime spectra were performed using an Edinburgh FS5 spectrophotometer with different detectors (Visible PMT and InGaAs 1650). The PLQY spectra at RT were carried out using this same fluorescence spectrometer. The PL spectra of NIR LEDs were recorded on fiber spectrophotometer. NIR photographs were taken by a computer equipped with a domestic USB NIR camera.

***PLQYs testing and calculation*:** To test the NIR PLQY of $Cs_2NaInCl_6$:Sb^{3+},Yb^{3+} and $Cs_2NaInCl_6$:Sb^{3+},Nd^{3+} samples, we used two detectors interchangeably (Visible PMT and InGaAs 1650). Taking $Cs_2NaInCl_6$:Sb^{3+},Nd^{3+} sample as an example. First, the visible (360~800 nm) PLQY of $Cs_2NaInCl_6$:Sb^{3+},Nd^{3+} sample was measured using a PMT detector and found to be 78.64%. Then, we used this detector to measure the PL spectrum from 360 nm to 1000 nm. Subsequently, an InGaAs 1650 detector was selected to test the NIR spectrum from 850 nm to 1500 nm. After measuring both spectra, the PL spectrum from 850 nm to 1000 nm measured by the PMT detector was normalized with the PL spectrum from 850 nm to 1000 nm measured by the InGaAs 1650 detector (Formula S1). After normalization, the ratio of the spectral area in the visible range (360~800 nm) to that in the NIR range (800~1500 nm) was determined to be S_1:S_2 = 1:0.1436 (Formula S2). Therefore, the NIR PLQY is estimated to be approximately 11.29% (Formula S3). And the PLQY of NIR emission from $Cs_2NaInCl_6$:Sb^{3+},Yb^{3+} sample has also undergone similar characterization tests. The specific calculations about $Cs_2NaInCl_6$:Sb^{3+},Nd^{3+} sample are as follows:

$$\frac{\int_{850\,nm}^{1000\,nm} I_{PMT}(\lambda)d\lambda}{\int_{850\,nm}^{1000\,nm} I_{InGaAs}(\lambda)d\lambda} = 1 \quad \text{(S1)}$$

$$\frac{S_1}{S_2} = \frac{\int_{360\,nm}^{800\,nm} I_{PMT}(\lambda)d\lambda}{\int_{800\,nm}^{1500\,nm} I_{InGaAs}(\lambda)d\lambda} = 1\text{: } 0.1436 \quad \text{(S2)}$$

$$\frac{PLQY_{Vis}}{PLQY_{NIR}} = \frac{S_1}{S_2} \rightarrow PLQY_{NIR} = PLQY_{Vis} \cdot \frac{S_2}{S_1} = 11.29\% \quad \text{(S3)}$$

***First principles calculations*:** We apply first-principles calculations based on density functional theory (DFT), implemented in the PWmat package using GPU[1,2]. In detail, the calculation of the structure and electronic properties, and defect properties of three structures are realized by PWmat. For the exchange-correlation potential, generalized gradient approximations (GGA)[3,4] of the Perdew-Burke-Ernzerhof (PBE) functional[5] is adopted and used in the geometry optimization with the force tolerance for the maximal residual force of $0.01eV$/Å as the convergence criteria. The PBE functional was also used for band structure, density of states and Charge density difference calculations. The Monkhorst-Pack k-points meshes of 0.04 /Å for geometry optimization. Norm-Conserving Pseudopotential[8,9] with a cutoff energy of 60 Rydberg have been used for all the calculations in the PWmat package.

Reference:

1. Jia, W. L.; Cao, Z. Y.; Wang, L.; Fu, J. Y.; Chi, X. B.; Gao, W. G.; Wang, L. W. *Comput. Phys. Commun.* **2013**, *184*, 9−18.

2. Jia, W. L.; Fu, J. Y.; Cao, Z. Y.; Wang, L.; Chi, X. B.; Gao, W. G.; Wang, L. W. *J. Comput. Phys.* **2013**, *251*, 102−115.

3. Perdew, J. P.; Burke, K.; Ernzerhof, M. *Phys. Rev. Lett.* **1996**, *77*, 3865.

4. Ziesche, P.; Kurth, S.; Perdew, J. P. *Comput. Mater. Sci.* **1998**, *11*, 122−127.

5. Perdew, J. P.; Burke, K.; Ernzerhof, M. *Phys. Rev. Lett.* **1996**, *77*, 3865−3868.

6. Heyd, J.; Scuseria, G. E.; Ernzerhof, M. *J. Chem. Phys.* **2003**, *118*, 8207−8215.

7. Krukau, A. V.; Vydrov, O. A.; Izmaylov, A. F.; Scuseria, G. E. *J. Chem. Phys.* **2006**, *125*, 224106.

8. Monkhorst, H. J.; Pack, J. D. *Phys. Rev. B* **1976**, *13*, 5188.

9. Hamann, D. R. *Phys. Rev. B* **2013**, *88*, 085117.

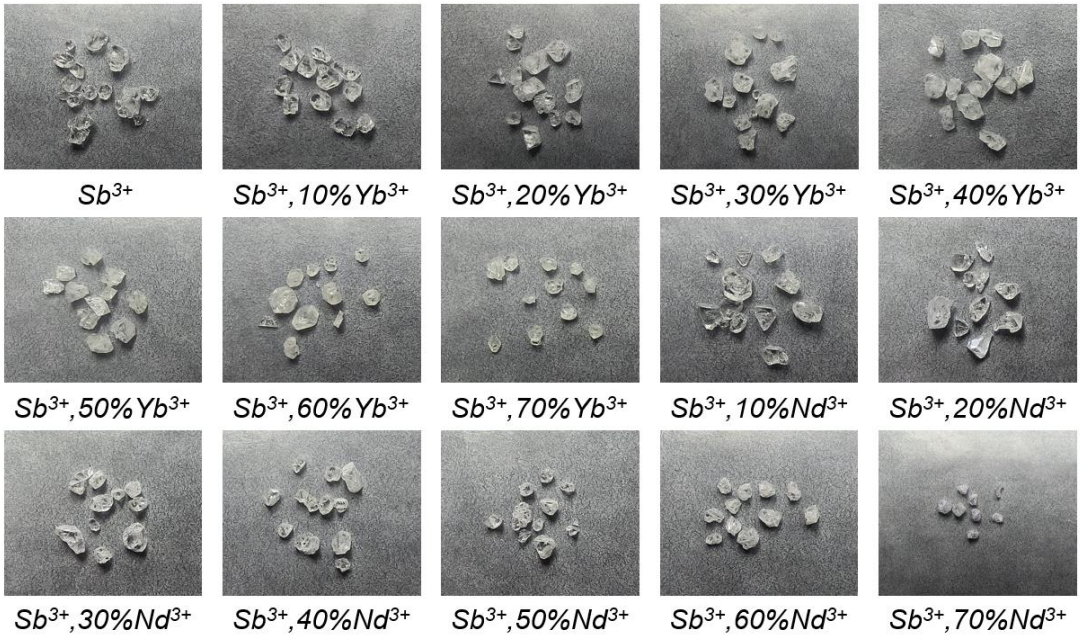

Figure S1. Photographs of $Cs_2NaInCl_6$:Sb^{3+}/Ln^{3+} single crystals under daylight.

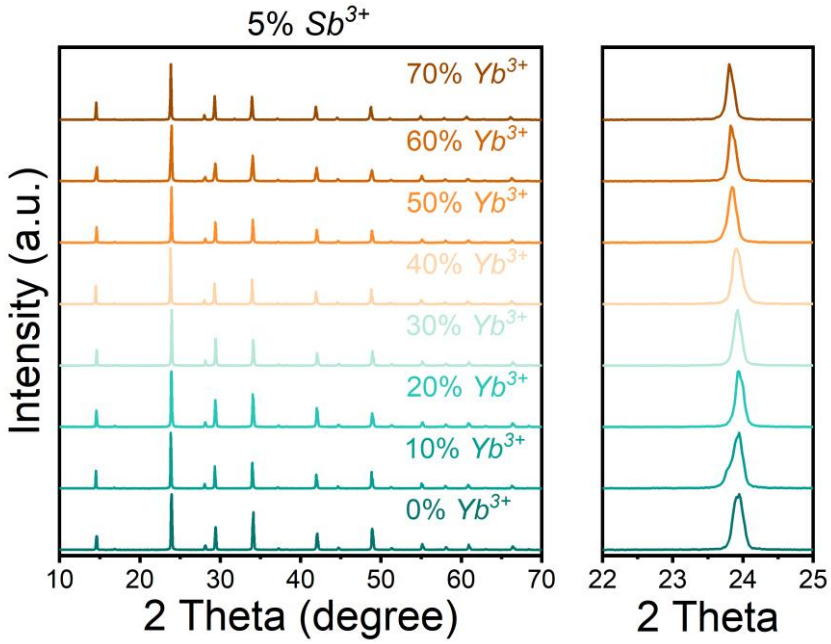

Figure S2. XRD patterns of $Cs_2NaInCl_6$:Sb^{3+}/Yb^{3+} with different Yb^{3+}-doping concentrations.

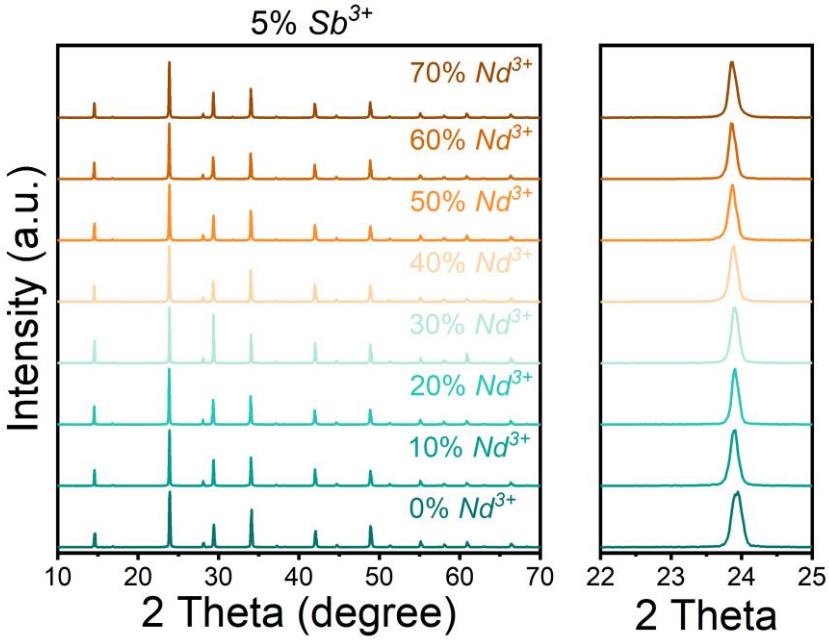

Figure S3. XRD patterns of $Cs_2NaInCl_6:Sb^{3+}/Nd^{3+}$ with different Nd^{3+}-doping concentrations.

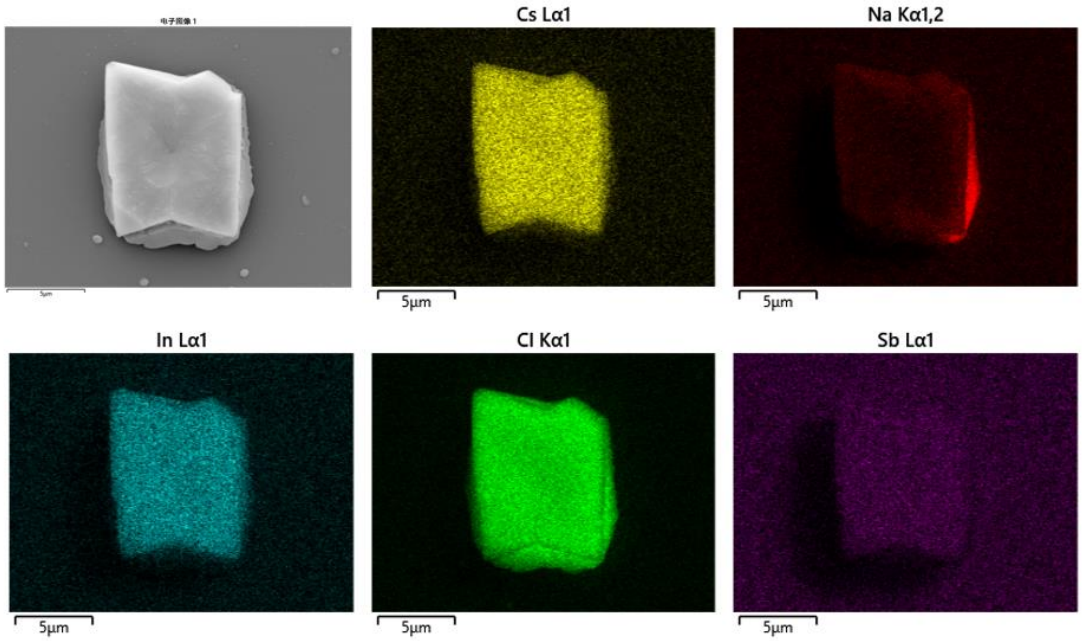

Figure S4. SEM image and EDX elemental mappings (Cs, Na, In, Cl, and Sb) of $Cs_2NaInCl_6:Sb^{3+}$ SCs.

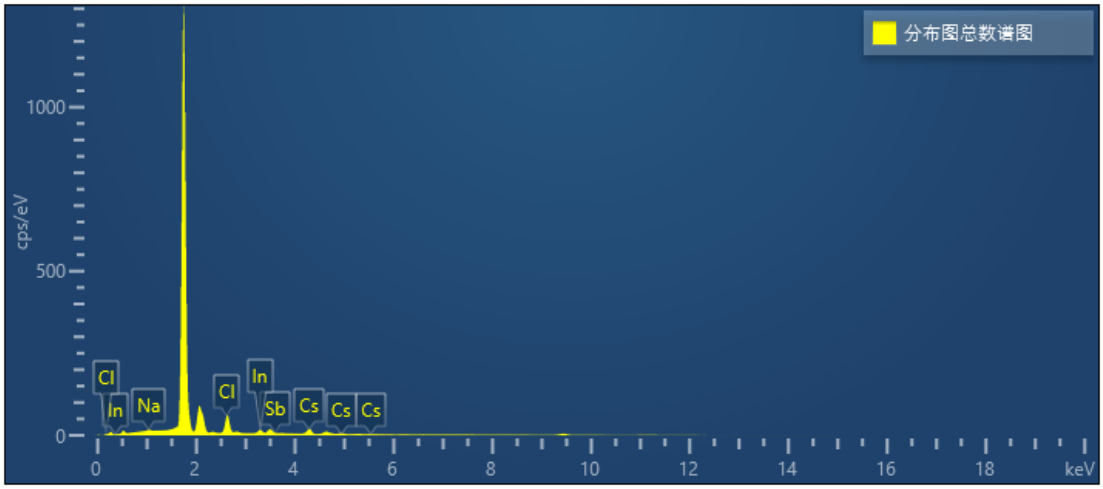

Figure S5. EDS spectra of $Cs_2NaInCl_6:Sb^{3+}$ sample.

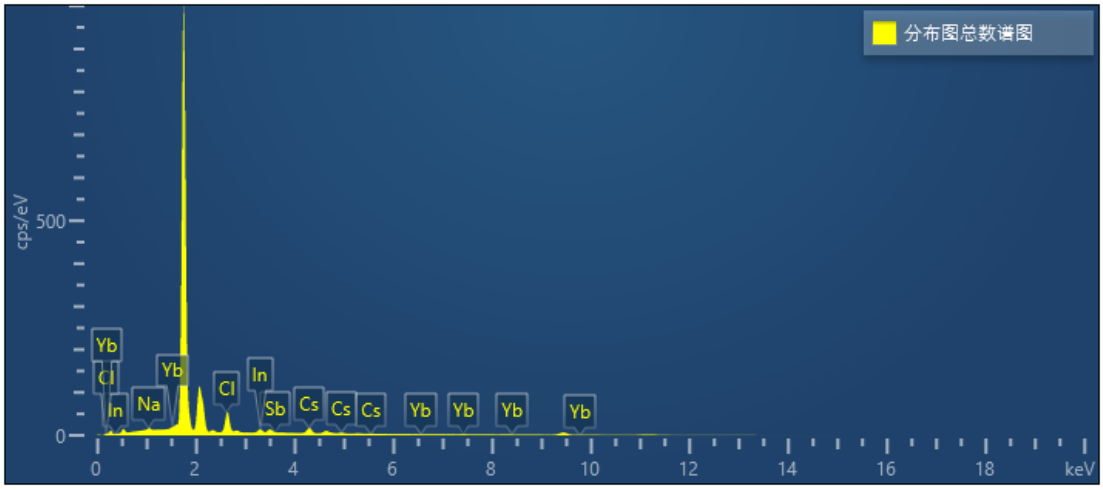

Figure S6. EDS spectra of $Cs_2NaInCl_6:Sb^{3+}/Yb^{3+}$ sample.

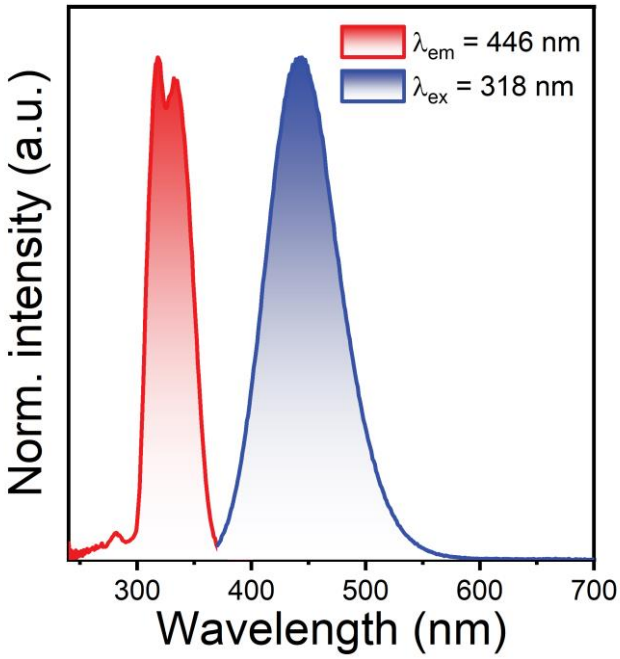

Figure S7. PL excitation (left, λ_{em} = 446 nm) and emission spectra (right, λ_{ex} = 318 nm) of $Cs_2NaInCl_6:Sb^{3+}$ SCs.

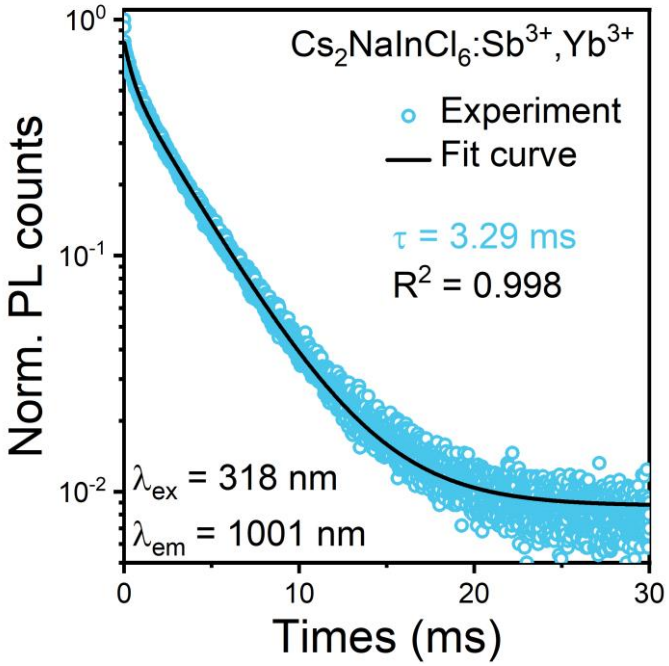

Figure S8. NIR PL decay time of $Cs_2NaInCl_6:Sb^{3+},Yb^{3+}$.

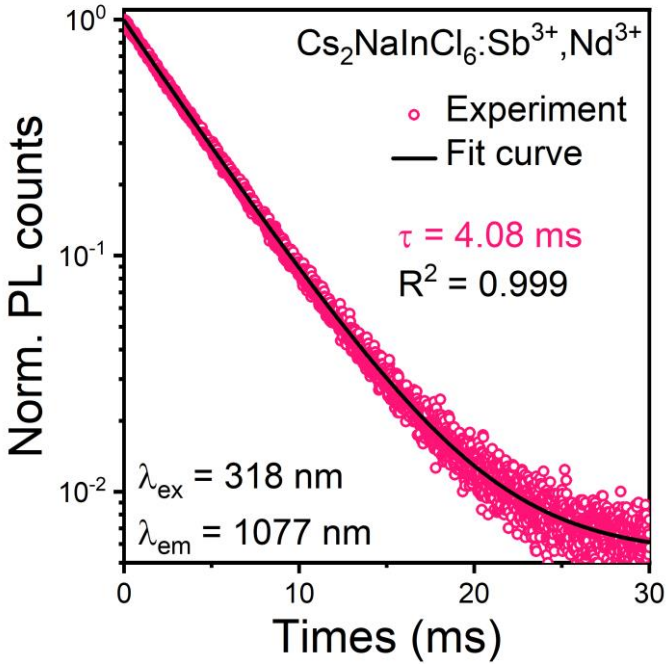

Figure S9. NIR PL decay time of $Cs_2NaInCl_6:Sb^{3+},Nd^{3+}$.

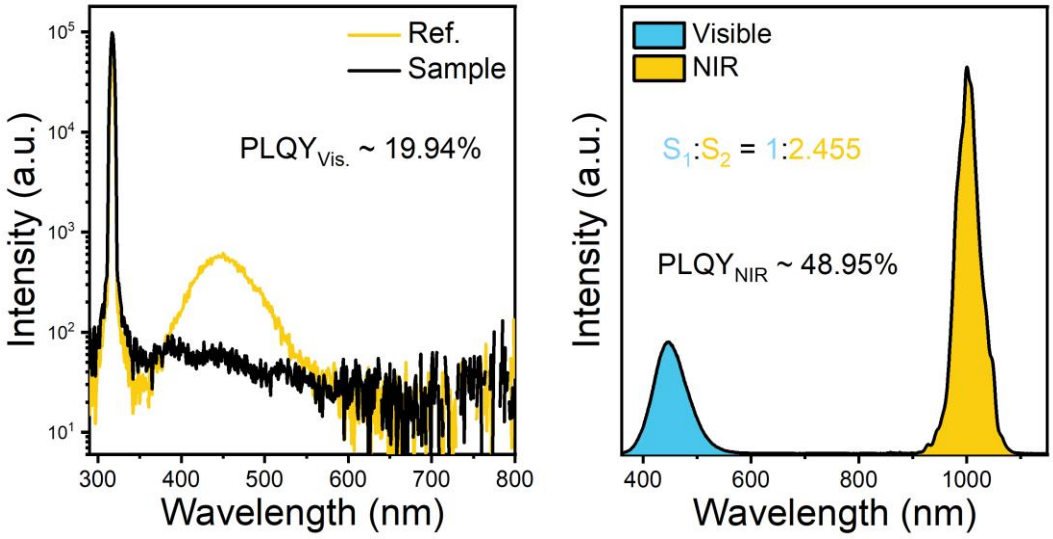

Figure S10. (Left) PLQY measurement of $Cs_2NaInCl_6:Sb^{3+},Yb^{3+}$ sample in the visible region. (Right) PL spectra of $Cs_2NaInCl_6:Sb^{3+},Yb^{3+}$ sample in whole range of 370-1150 nm, and the integrated intensity of NIR to visible emission is calculated to be 2.455.

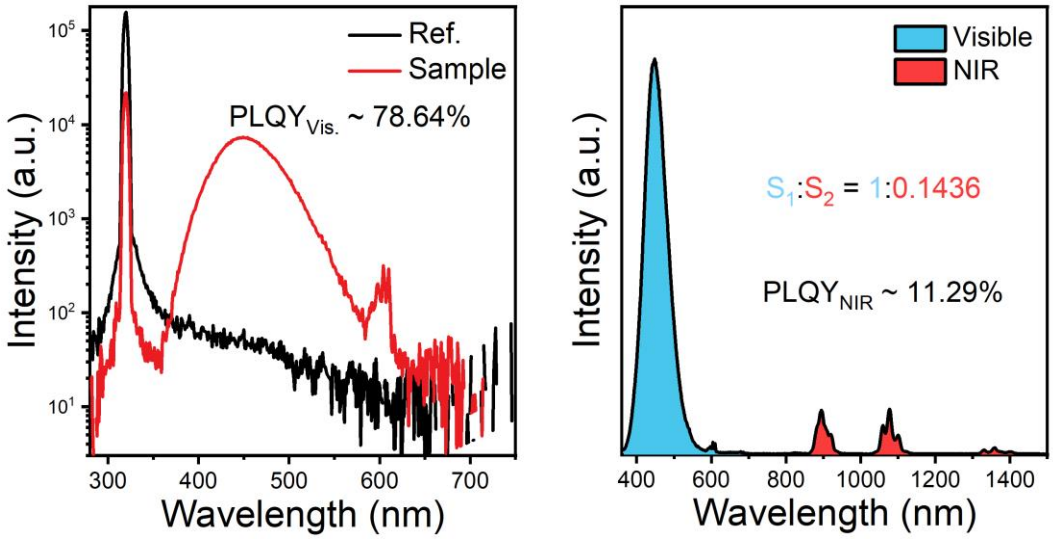

Figure S11. (Left) PLQY measurement of $Cs_2NaInCl_6:Sb^{3+},Nd^{3+}$ sample in the visible region. (Right) PL spectra of $Cs_2NaInCl_6:Sb^{3+},Nd^{3+}$ sample in whole range of 370-1500 nm, and the integrated intensity of NIR to visible emission is calculated to be 0.1436.

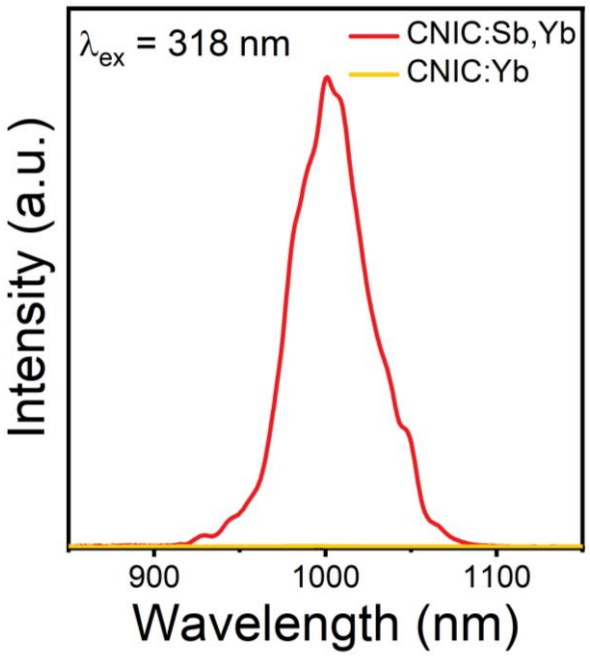

Figure S12. NIR PL spectra of $Cs_2NaInCl_6:Yb^{3+}$ and $Cs_2NaInCl_6:Sb^{3+},Yb^{3+}$ respectively.

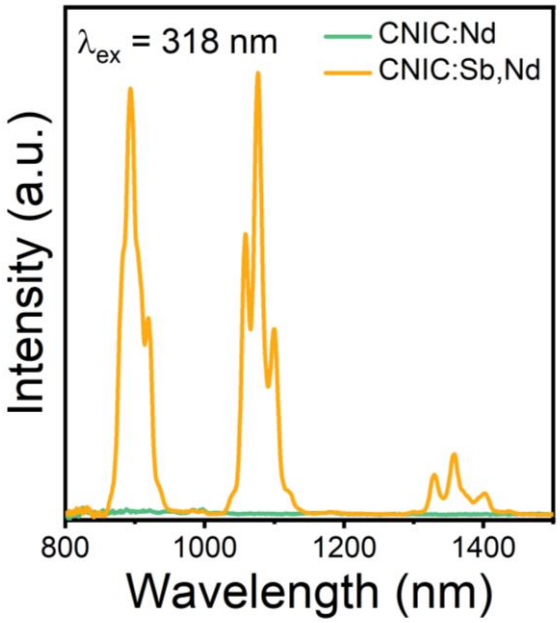

Figure S13. NIR PL spectra of $Cs_2NaInCl_6:Nd^{3+}$ and $Cs_2NaInCl_6:Sb^{3+},Nd^{3+}$ respectively.

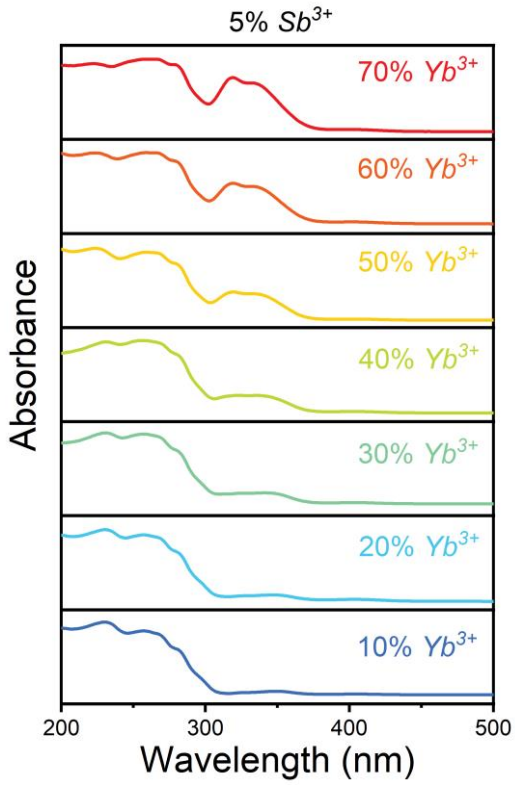

Figure S14. Ultraviolet–visible absorption spectra of $Cs_2NaInCl_6:Sb^{3+},Yb^{3+}$ samples with increased Yb^{3+} dopant levels.

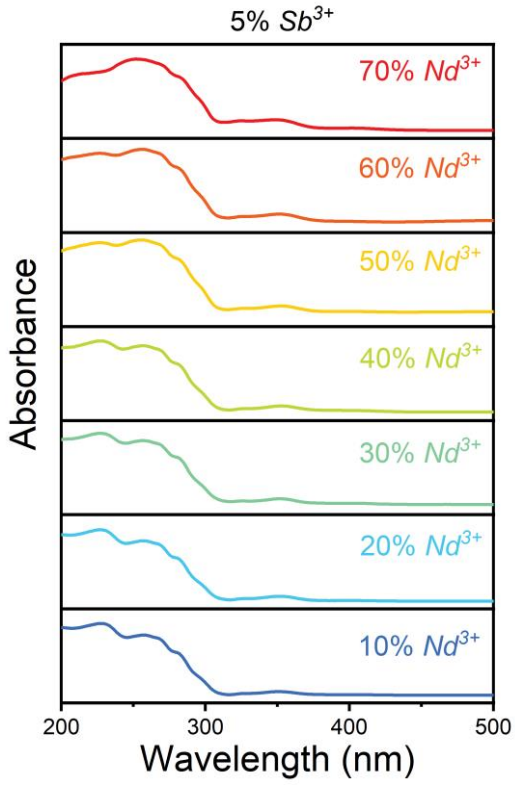

Figure S15. Ultraviolet–visible absorption spectra of $Cs_2NaInCl_6:Sb^{3+},Nd^{3+}$ samples with increased Nd^{3+} dopant levels.

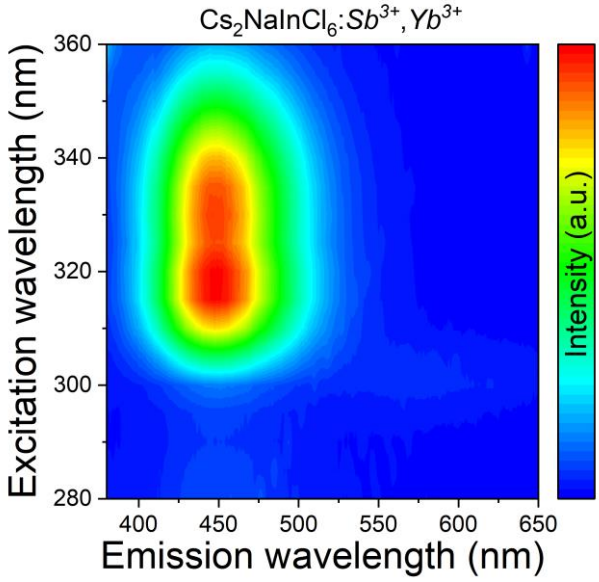

Figure S16. PL and PLE mapping of $Cs_2NaInCl_6:Sb^{3+},Yb^{3+}$ at room temperature.

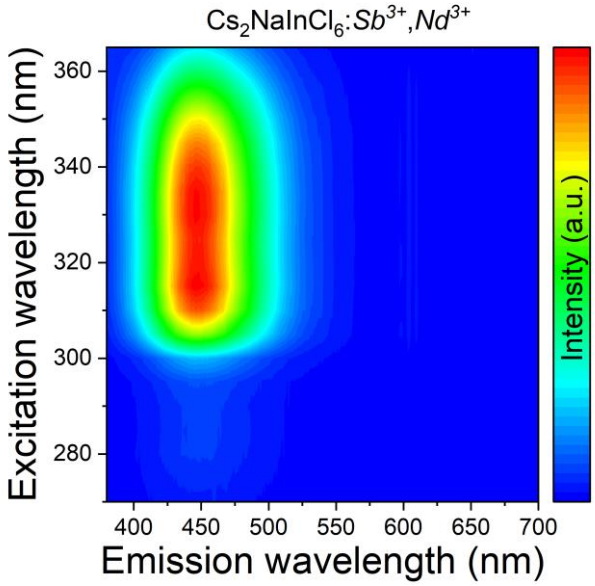

Figure S17. PL and PLE mapping of $Cs_2NaInCl_6:Sb^{3+}$, Nd^{3+} at room temperature.

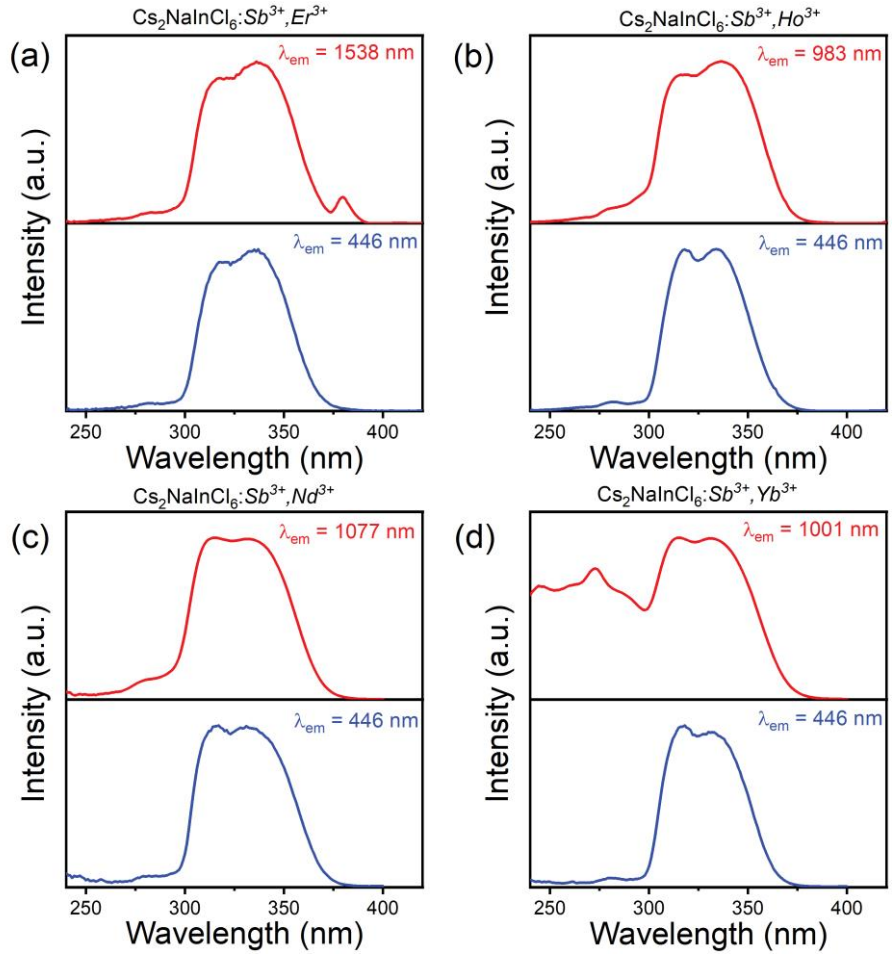

Figure S18. PLE spectra of (a) $Cs_2NaInCl_6:Sb^{3+}$, Er^{3+}; (b) $Cs_2NaInCl_6:Sb^{3+}$, Ho^{3+}; (c) $Cs_2NaInCl_6:Sb^{3+}$, Nd^{3+}; and (d) $Cs_2NaInCl_6:Sb^{3+}$, Yb^{3+}.

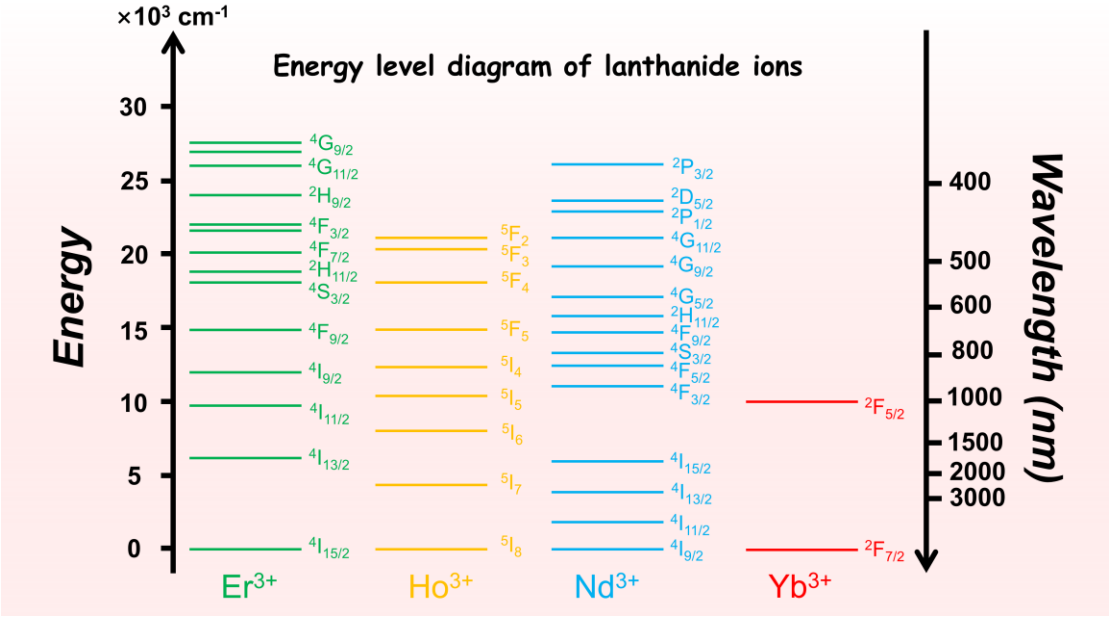

Figure S19. Energy-level diagrams of the Er^{3+}, Ho^{3+}, Nd^{3+}, and Yb^{3+} ions.

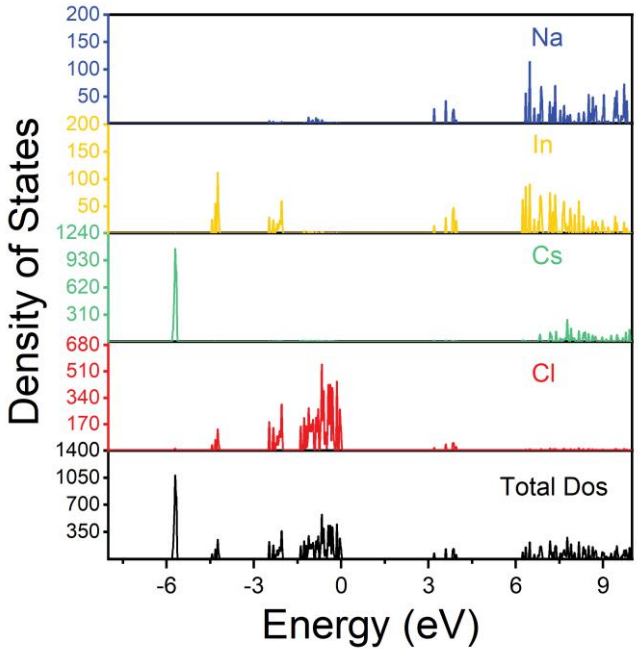

Figure S20. The total and partial density of states of $Cs_2NaInCl_6$.

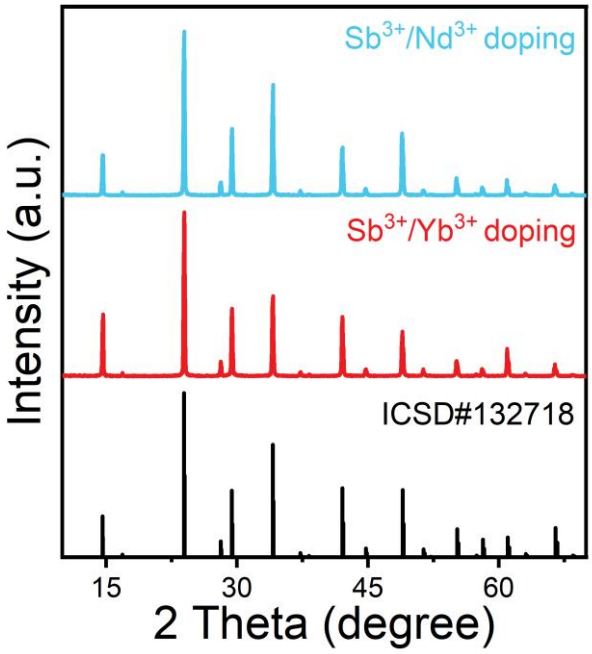

Figure S21. PXRD patterns of $Cs_2NaInCl_6$:Sb^{3+}/Ln^{3+} after the continuous illumination under a 365 nm ultraviolet light.

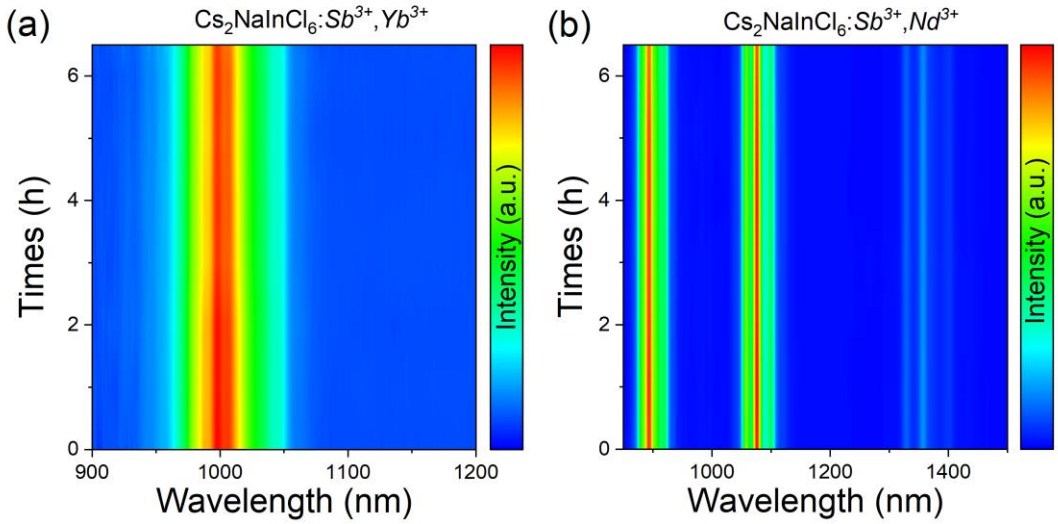

Figure S22. The PL-temperature correlation maps of (a) $Cs_2NaInCl_6$:Sb^{3+}/Yb^{3+} and (b) $Cs_2NaInCl_6$:Sb^{3+}/Nd^{3+} maintained at 420 K for 6.5 h.

Table S1. ICP elemental analysis of $Cs_2NaInCl_6$:Sb/Yb.

Sample	$Cs_2NaInCl_6:Sb^{3+}/Yb^{3+}$			
	Feeding ratio		Actual	
	Sb^{3+}	Yb^{3+}	Sb^{3+}	Yb^{3+}
1	5%	10%	0.0978%	0.1603%
2	5%	20%	0.1177%	0.2862%
3	5%	30%	0.1815%	0.8067%
4	5%	40%	0.2455%	1.7652%
5	5%	50%	0.2721%	2.8759%
6	5%	60%	0.4916%	7.0861%
7	5%	70%	0.7028%	10.9443%

Table S2. ICP elemental analysis of $Cs_2NaInCl_6$:Sb/Nd.

Sample	$Cs_2NaInCl_6:Sb^{3+}/Nd^{3+}$			
	Feeding ratio		Actual	
	Sb^{3+}	Nd^{3+}	Sb^{3+}	Nd^{3+}
8	5%	10%	0.1355%	0.0049%
9	5%	20%	0.1761%	0.0111%
10	5%	30%	0.1850%	0.0179%
11	5%	40%	0.2262%	0.0279%
12	5%	50%	0.2721%	0.0584%
13	5%	60%	0.3828%	0.0881%
14	5%	70%	0.5580%	0.2211%

Table S3. ICP and EDS elemental analysis of $Cs_2NaInCl_6$:Sb/Yb sample.

Sample	ICP-MS		EDS	
	Sb^{3+}	Yb^{3+}	Sb^{3+}	Yb^{3+}
$Cs_2NaInCl_6$:5%Sb^{3+}/40%Yb^{3+}	0.2455%	1.7652%	0.2108%	1.5729%

Table S4. PL performance of near-infrared metal halides.

Host	Doped Ion	Morphology	NIR PLQY	Ref.
$Cs_2AgInCl_6$	Cr^{3+}	phosphor	22.03%	10
$Cs_2AgInCl_6$	Yb^{3+}	NCs	3.6%	11
$Cs_2AgInCl_6$	Sb^{3+}/Yb^{3+}	SCs	50%	12
$Cs_2AgBiBr_6$	Yb^{3+}	film	28%	13
$Cs_2Ag_{0.2}Na_{0.8}BiCl_6$	Yb^{3+}	NCs	19%	14
$Cs_3Bi_2Br_9$	Yb^{3+}	film	14.5%	15
Cs_2ZrCl_6	Te^{4+}/Er^{3+}	MCs	6.1%	16
$Cs_2NaInCl_6$	Yb^{3+}	SCs	39.4%	17
$Cs_2NaInCl_6$	Sb^{3+}/Yb^{3+}	SCs	48.95%	This work
$Cs_2NaInCl_6$	Sb^{3+}/Nd^{3+}	SCs	11.29%	This work

Table S5. The PL lifetimes of $Cs_2NaInCl_6$:Sb/Yb monitored at 446 nm.

Sample	Lifetimes (μs)	η_T
2116: Sb	1.82	/
2116: Sb/Yb (0.1603%)	1.79	1.65%
2116: Sb/Yb (0.2862%)	1.75	3.85%
2116: Sb/Yb (0.8067%)	1.74	4.40%
2116: Sb/Yb (1.7652%)	1.63	10.44%
2116: Sb/Yb (2.8759%)	1.59	12.64%
2116: Sb/Yb (7.0861%)	1.47	19.23%
2116: Sb/Yb (10.9443%)	1.02	43.96%

Table S6. The PL lifetimes of $Cs_2NaInCl_6$:Sb/Nd monitored at 446 nm.

Sample	Lifetimes (μs)	η_T
2116: Sb	1.796	/
2116: Sb/Nd (0.0049%)	1.743	2.95%
2116: Sb/Nd (0.0111%)	1.741	3.06%
2116: Sb/Nd (0.0179%)	1.736	3.34%
2116: Sb/Nd (0.0279%)	1.732	3.56%
2116: Sb/Nd (0.0584%)	1.718	4.34%
2116: Sb/Nd (0.0881%)	1.703	5.18%
2116: Sb/Nd (0.2211%)	1.692	6.35%

References

10. Zhao, F. Y.; Song, Z.; Zhao, J.; Liu, Q. L. *Inorg. Chem. Front.* **2019**, *6*, 3621–3628.

11. Lee, W.; Hong, S.; Kim, S. *J. Phys. Chem. C* **2019**, *123*, 2665–2672.

12. Cao, L. Y.; Jia, X. F.; Gan, W. J.; Ma, C. G.; Zhang, J. Y.; Lou, B. B.; Wang, J. *Adv. Funct. Mater.* **2023**, *33*, 2212135.

13. Schmitz, F.; Guo, K.; Horn, J.; Sorrentino, R.; Conforto, G.; Lamberti, F.; Brescia,

R.; Drago, F.; Prato, M.; He, Z.; Giovanella, U.; Cacialli, F.; Schlettwein, D.; Meggiolaro, D.; Gatti, T. *J. Phys. Chem. Lett.* **2020**, *11*, 8893.

14. Pei, Y.; Tu, D.; Li, C.; Han, S.; Xie, Z.; Wen, F.; Wang, L.; Chen, X. *Angew. Chem. Int. Ed.* **2022**, *61*, 202205276.

15. Tran, M. N.; Cleveland, I. J.; Pustorino, G. A.; Aydil, E. S. *J. Mater. Chem. A* **2021**, *9*, 13026.

16. Sun, J. Y.; Zheng, W.; Huang, P.; Zhang, M. R.; Zhang, W.; Deng, Z. H.; Yu, S. H.; Jin, M. Y.; Chen, X. Y. *Angew. Chem. Int. Ed.* **2022**, *61*, e202201993.

17. Han, S. Y.; Tu, D. T.; Xie, Z.; Zhang, Y. Q.; Li, J. Y.; Pei, Y. F.; Xu, J.; Gong, Z. L.; Chen, X. Y. *Adv. Sci.* **2022**, *9*, 2203735.